Combustion Stability Characteristics of the Project Morpheus Liquid Oxygen / Liquid Methane Main Engine

John C. Melcher[*] and Robert L. Morehead[†]

NASA Johnson Space Center, Houston, TX, 77058, United Sates

   The project Morpheus liquid oxygen (LOX) / liquid methane (LCH4) main engine is a Johnson Space Center (JSC) designed ~5,000 lbf-thrust, 4:1 throttling, pressure-fed cryogenic engine using an impinging element injector design. The engine met or exceeded all performance requirements without experiencing any in-flight failures, but the engine exhibited acoustic-coupled combustion instabilities during sea-level ground-based testing. First tangential (1T), first radial (1R), 1T1R, and higher order modes were triggered by conditions during the Morpheus vehicle derived low chamber pressure startup sequence. The instability was never observed to initiate during mainstage, even at low power levels. Ground-interaction acoustics aggravated the instability in vehicle tests. Analysis of more than 200 hot fire tests on the Morpheus vehicle and Stennis Space Center (SSC) test stand showed a relationship between ignition stability and injector/chamber pressure. The instability had the distinct characteristic of initiating at high relative injection pressure drop at low chamber pressure during the start sequence. Data analysis suggests that the two-phase density during engine start results in a high injection velocity, possibly triggering the instabilities predicted by the Hewitt stability curves. Engine ignition instability was successfully mitigated via a higher-chamber pressure start sequence (e.g., ~50% power level vs ~30%) and operational propellant start temperature limits that maintained "cold LOX" and "warm methane" at the engine inlet. The main engine successfully demonstrated 4:1 throttling without chugging during mainstage, but chug instabilities were observed during some engine shutdown sequences at low injector pressure drop, especially during vehicle landing.

Nomenclature

A	Injector face orifice area total for a given propellant, sq.in.
C	Chisholm empirical constant
C_d	Discharge coefficient
$C*$	Characteristic velocity, ft/sec
d	Injector orifice diameter, inches
d/v	Injector Hewitt stability parameter, sec
K	Chisholm empirical constant
$\dot{m}$	Propellant mass flow rate, lbm/sec
Pc	Chamber pressure, psig
Q	Propellant volumetric flow rate, cu.ft./sec
v	Injection velocity, ft/sec
X	Two-phase Lockhart-Martinelli parameter
x	Two-phase fluid quality, $x = 0$ at saturated liquid, $x = 1$ at saturated vapor
ΔP	Injector pressure drop, psid
$\Delta P/Pc$	Injector pressure drop / chamber pressure ratio, psid/psia
ρ	Propellant density, lbm/cu.ft.

---

[*]Liquid Propulsion Systems Engineer, Propulsion and Power Division, AIAA Senior Member.
[†]Liquid Propulsion Systems Engineer, Propulsion and Power Division, AIAA Member.

American Institute of Aeronautics and Astronautics

Subscripts
g   gas (vapor) phase
l   liquid phase
2ϕ two-phase

Acronyms

AES	Advanced Exploration Systems
ALHAT	Automated Landing and Hazard Avoidance Technology
E3	Stennis Space Center Test Stand E3
FFC	Fuel-film Cooling
GNC	Guidance, Navigation, and Control
HD	Morpheus main engine moniker (e.g., HD4, HD4-A, HD4-A-LT, HD4-B-LT, HD5)
HEOMD	Human Exploration Operations Mission Directorate
ISRU	In-situ Resource Utilization
JSC	Johnson Space Center
KSC	Kennedy Space Center
LCH4	Liquid Methane
L	Longitudinal mode
LNG	Liquefied Natural Gas
LOL	Like-on-like doublet
LOX	Liquid Oxygen
LT	Large Throat
PSD	Power Spectral Density
R	Radial mode
RCE	Reaction Control Engine
SSC	Stennis Space Center
SSC − E3	Stennis Space Center Test Stand E3
T	Tangential mode
1R, 2R, 3R	First Radial, Second Radial, Third Radial
1T, 2T, 3T	First Tangential, Second Tangential, Third Tangential
1T1R, 1T2R	First Tangential-Radial, Second Tangential-Radial

I.   Introduction

Project Morpheus is a test bed for integrating and demonstrating technologies for planetary lander-class vehicles. Project Morpheus is part of the NASA Human Exploration Operations Mission Directorate (HEOMD) Advanced Exploration Systems (AES) programs. Morpheus was designed, built, and tested at NASA Johnson Space Center (JSC). Vertical takeoff and landing tests of the Morpheus vehicle under tethered constraint were conducted at JSC, and free-flight high altitude tests were conducted at Kennedy Space Center (KSC), shown in Figure 1. To date, Morpheus has successfully completed 13 free-flight demonstrations at KSC and 36 tethered tests at JSC and KSC. Standalone main engine checkout and qualification testing was conducted at Stennis Space Center (SSC) on test stand E-3.

Morpheus utilizes a liquid oxygen/liquid methane propulsion system with integrated reaction control engine (RCE), main engine, propellant tanks, and feedsystems (i.e., common commodities from common tanks). The vehicle contains its own on-board power and avionics systems, including fully-automated guidance, navigation, and control systems (GNC). In 2014, Project Morpheus successfully demonstrated fully autonomous flight and landing into a debris field using the Automated Landing and Hazard Avoidance Technology (ALHAT) system. Further details and discussion of the Project Morpheus can be found in references 1 and 2.

Project Morpheus uses LOX/methane propulsion in order to further the technology needed for lunar and Mars lander vehicles of future missions. Multiple NASA mission architecture studies have identified LOX/methane as the recommended propulsion system for the lander vehicle due to its increased performance and eliminated toxicity compared to conventional hypergolic "storable" propellants. LOX/methane

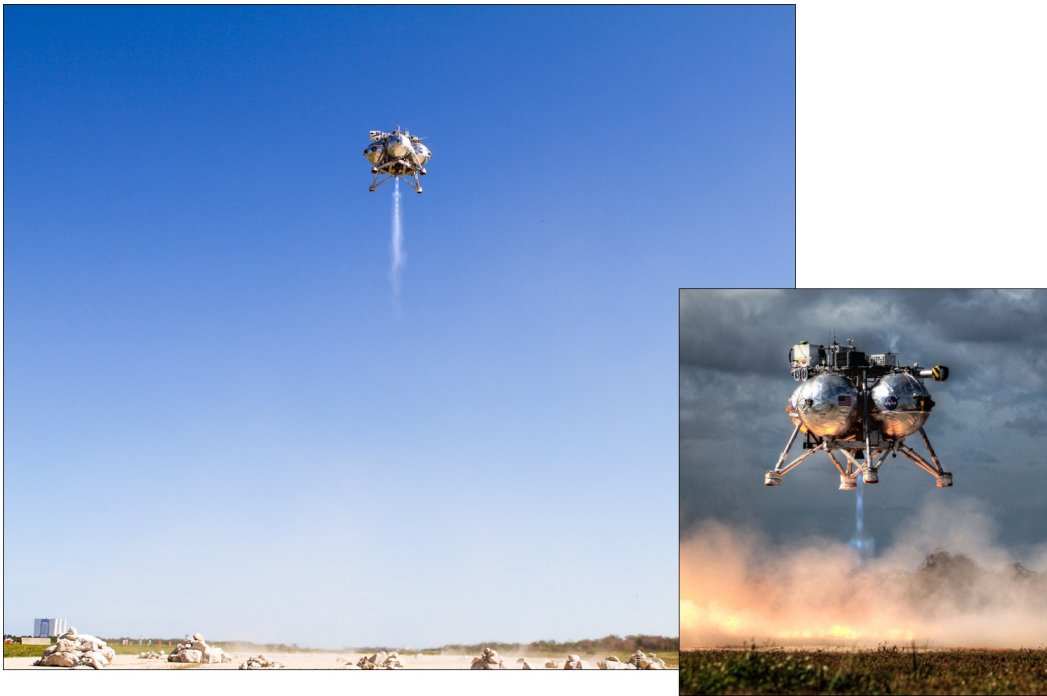American Institute of Aeronautics and Astronautics

Figure 1. Morpheus vehicle free-flight demonstration at KSC.

offers size and volume improvements for landers compared with oxygen-hydrogen propulsion. LOX/methane propulsion also utilizes synergy with in-situ resource utilization (ISRU) technologies that have the potential to produce oxygen and methane propellant from lunar regolith or Mars environments. Lastly, oxygen-methane propulsion systems reduce overall vehicle design complexity and inert mass by utilizing commodities common with other vehicle systems (e.g., oxygen for life-support systems, methane for solid-oxide fuel cell power systems).

Integrated main engine and reaction control engine (RCE) operation from common tanks was demonstrated on the Morpheus lander. The 5-20 lbf RCEs provide roll control of the vehicle during flight. Additional details on the Morpheus reaction control engines may be found in references 3 and 4.

II.   Morpheus Main Engine Design and Test Overview

The Project Morpheus main engines were designed and fabricated in-house at NASA-JSC, utilizing the nomenclature HD3, HD4, and HD5. The engines generally have grown in designed thrust capability, with the final flight configurations reaching ~5,400 lbf-sea-level maximum thrust at 109% power level. The engines have demonstrated a 4:1 deep throttling capability, which enabled the lander operations, giving an overall throttle range of 25% - 109%. Testing was conducted at JSC and KSC on the Morpheus vehicle, and at SSC on test stand E-3, shown in Figure 2.

For all testing, liquefied natural gas (LNG) was used as the liquid methane (LCH4) propellant. Quality samples were measured for each load, and methane purity was consistently greater than 99%, with hydrocarbons comprising most of the residual.

The engines use a like-on-like (LOL) impinging element injector faceplate design and the chamber/nozzle is cooled with fuel film cooling (FFC), up to 30% of the total fuel flow. The high-FFC design traded engine specific impulse efficiency for manufacturability and design costs.

A notable engine design artifact relevant to this work is the main throttle valve assembly. The Morpheus main engines use a common valve actuator for both inlet propellant ball valves, rotating them symmetrically. This design selection was made to reduce failure modes in the vehicle, but had consequences that the engine mixture ratio could not be actively controlled and the valves could not be commanded independently during the start sequence. Additional design heritage of the Morpheus main engine is described in reference 5.

American Institute of Aeronautics and Astronautics

Engines HD1 and H3 were the initial engines used in early vehicle configuration testing (2010-2011). All subsequent vehicle testing utilized the HD4 engine configuration, and multiple versions of HD4 were tested and flown. HD5 was tested at SSC, but never flown on the vehicle due to thermal issues during development.

The HD4 engine was tested and flown in multiple configurations. The first Morpheus vehicle for free-flight testing, vehicle 1.5a, used the original HD4 engine (HD4-A) in its baseline configuration of 4,200 lbf thrust. This was the configuration flown during the first round of free-flight demonstrations at KSC in 2012, which resulted in a catastrophic vehicle failure due loss of navigation and control data.[1] Mass growth of the next Morpheus vehicle, Vehicle 1.5b, and of the ALHAT payload required a higher thrust engine to support the required mission duration. Hence, the higher thrust/higher efficiency HD5 engine was developed. This engine had initial troubles with film cooling and was the first engine to experience unstable ignitions at SSC, beginning the analysis effort outlined in this paper. The HD4-A injector was salvaged from the Vehicle 1.5a wreckage and was reconfigured for use on the heavier Morpheus 1.5b flights. By outfitting this injector with a "large-throat" chamber, the max thrust was increased to 5,000 lbf and later pushed to 5,400 lbf, allowing the updated HD4-A-LT engine to fly all 2013 and 2014 Morpheus 1.5b flights at JSC and KSC (to date). A second HD4 engine was built and tested at SSC-E3 in the large throat configuration, with the nomenclature HD4-B-LT, but has not yet flown on the Morpheus vehicle. A summary of the engine configurations tested at SSC and on the vehicle is shown in Table 1.

Figure 2. Morpheus Main Engine Testing at SSC test stand E-3, with nozzle exit and flame trench inlet in close proximity.

The Morpheus main engine successfully met or exceeded its performance requirements and demonstrated 4:1 throttling, enabling Project Morpheus success. The main engines never experienced a in-flight failure during Morpheus flights. Several issues were overcome during development testing, including startup combustion instabilities, but the operational flight objectives were ultimately achieved with safe and reliable main engine performance.

A.   Engine Start Sequence on the Morpheus Vehicle

Prior to launch, the Morpheus vehicle rested unsecured on three collapsible launch stands, with integrated load cells on the vehicle providing real-time weight and center of gravity measurements until the moment of launch. The vehicle's four legs hung from the vehicle in this configuration, without a hold-down mechanism. During the engine ignition sequence, the engine was throttled from zero thrust to an "idle" thrust state, where the engine was producing much less thrust than the vehicle weighed at that time, preventing premature lift-off or shifting on the launch stands. During this idle state, the flight software transitioned control of the main engine from Propulsion sequencing to GNC flight control. Once in control, the GNC flight software commanded a near maximum thrust level, targeting a 1.15g liftoff acceleration, resulting in vehicle launch. This two-step ignition sequence (ignition to idle thrust then idle to max thrust) allowed for verification of engine health prior to flight followed by a smooth transition from a stationary state to an active flight phase. Without a hold-down mechanism, igniting the engine directly into the max thrust state would have turned engine ignition risk into flight risk. Additionally, possible asymmetric thrust during ignition (or

American Institute of Aeronautics and Astronautics

Table 1. Morpheus main engine configuration summary

Engine Name	HD4-A (baseline)	HD4-A-LT (large throat)	HD4-B-LT (large throat)	HD5
Test Years	2012	2012-2014	2013-2014	2012-2013
Thrust (lbf)	4,200	5,400	5,400	5,400+
Vehicle Test Starts	19	73	n/a	n/a
Vehicle Cum. Run Time (sec)	841	1,871	n/a	n/a
Vehicle Tests with Instability	0	17	n/a	n/a
SSC Test Starts	n/a	26	22	66
SSC Test Cum. Run Time (sec)	n/a	216	400	165
SSC Tests with Instability	n/a	11	0	22

other types of unplanned ignition anomalies) would become vehicle motion that the GNC system would have to immediately overcome as the flight phase began. Hence, operating the developmental engine and developmental GNC systems in a single ignition-to-flight step would have been more risky than separating them into individual stages via the two step ignition sequence.

In early engine testing, it was found that the engine lit more smoothly with a strong liquid oxygen lead. Lighting the engine with both liquid oxygen and liquid methane in the injector typically resulted in unreliable mixture ratios during start, including stronger pulses and in some cases bangs at the onset of chamber pressure. Since the engine main valves are driven symmetrically via a single actuator, mixture ratio cannot be actively controlled during the ignition sequence or during mainstage. Therefore, in order to start the engine with a liquid oxygen lead (facilitating smooth ignitions) the Morpheus liquid oxygen feedline and the liquid oxygen half of the main engine injector were pre-chilled to near-liquid cryogenic conditions, whereas the methane feedline and injector manifold were pre-chilled, but not to cryogenic conditions. This effectively caused a liquid oxygen lead during the ignition sequence with symmetric main ball valve actuation.

Igniting the engine into the low thrust idle state with the asymmetric feedline pre-chill typically resulted in an intermediate thrust pause during the thrust increase from zero to idle. The initial onrush of gaseous and two phase propellants increased the chamber pressure from zero to the pause point of intermediate power level, typically around 30% power level. As both propellant manifolds transitioned into a sub-cooled propellant state, the chamber pressure would rise to the true idle power level of ~50% for the handover of engine control from Propulsion to GNC (see Figure 3).

The power level of the intermediate pause state became a driving factor in the initiation and resolution of the instability issue described in this paper. Early in the Morpheus engine development the power level for idle was set at a maximum of ~50% of the vehicle weight, without consideration for the two-step transition period from zero thrust to idle. This sequencing approach was maintained until the large throat version of the HD4 engine (HD4-A-LT) was tested on the vehicle, and the instability issues during this two-step transition period were discovered.

Two operational changes to the pre-chill and ignition sequence essentially eliminated the ignition instability issues. First, the power level of the intermediate pause and idle states were increased to force the engine to reach a higher chamber pressure level more quickly thereby decreasing the timeframe of exposure to high two-phase orifice velocities. Second, the methane feedline/engine manifold was maintained at near room temperature until engine ignition (e.g. "warm methane") and the liquid oxygen pre-chill timeframe was extended, thereby maximizing the liquid oxygen lead during the ignition sequence.

The Morpheus team was called upon to create a requirement for maximum engine thrust during the prelaunch idle timeframe, and determined that the engine should produce no more force than 70% of the vehicle weight at that time. This requirement ensured the vehicle would remain seated on the launch stands during the ignition sequence and would only move when the max thrust liftoff command was sent by the GNC software.

Hence, the revised ignition sequence resulted in an increase of the intermediate pause power level from ~30% to ~50%, and the final idle power level was increased from ~50% to ~60%. This change reduced the

American Institute of Aeronautics and Astronautics

typical ignition sequence duration from ˜1 sec to ˜0.5 sec (from zero to idle thrust).
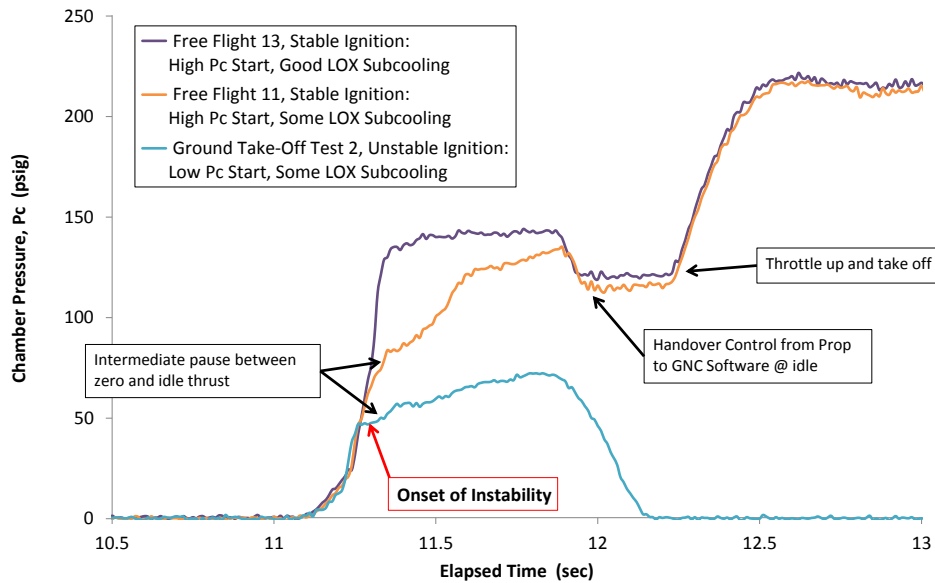

Figure 3. Morpheus main engine start sequence improvements

B.   Acoustic Cavity Design Overview

The HD4 and HD5 engines were designed with acoustic cavity damping devices for high-speed combustion instability protection. The cavities were designed as 1/4 wave tubes, intended to protect for the 1T, 2T and 3T modes of the chamber. The cavity ring is integral to the injector manifold, mounted 45 degrees offset between the chamber wall and the face, shown in Figure 4(a). The cavity design included 21 dedicated cavities in a ring of 24 tubes, and the cavity area was approximately 16-17% of the injector face area. The additional cavity locations were used for high speed pressure measurement and igniter ports.

Figure 4. Morpheus main engine injector acoustic cavity layout. (a) Acoustic cavity ring at 45 deg to faceplate. (b) Tunable acoustic cavity configuration.

The cavities were constructed of pipe segments mounted adjacent to the injector with large and small internal plungers on threaded rods, shown in Figure 4(b). The plunger design allowed for the cavity depths

American Institute of Aeronautics and Astronautics

to be adjusted during checkout testing. For the flight configuration and testing, the cavities were fixed length. Tuning of the cavities was accomplished by measuring cavity temperatures with a thermocouple rake installed in short and long cavities. A non-linear drop in gas temperature (and assumed sound speed) was observed down the length of the cavity, variable with total cavity length, as shown in Figure 5.

Although the cavities were originally designed to have a sharp-edge entrance, the resultant test hardware used a less ideal rounded entrance. The rounding resulted from a combination of the welding process of the cavity tubes into the injector, and erosion/repair of the sharp edges during hot-fire testing.

C. Main Engine Instrumentation

The Morpheus main engine included both high speed and low-speed instrumentation. Low-speed data (chamber and injector pressures, temperatures, and flow rates) was recorded through the Morpheus vehicle flight computer at 100 Hz, both on the vehicle and on the test stand. High-speed data (dynamic pressure, accelerometer) was recorded through standalone systems, using different systems for the vehicle and test stand.
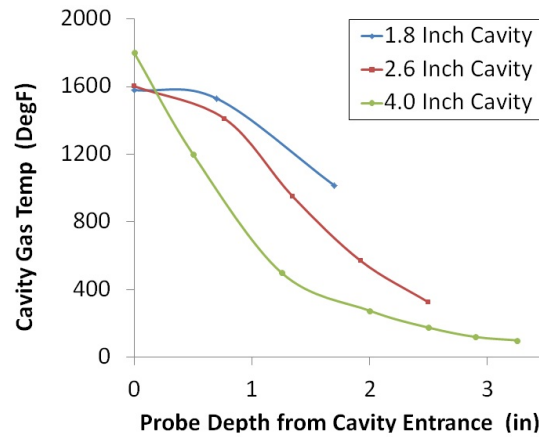
Figure 5. Example Cavity Gas Temperatures.

1. Low-speed Instrumentation

Low-speed pressure data was recorded for chamber pressure (Pc), LOX injector pressure, LCH4 injector pressure, igniter pressure, and other locations. Low speed pressure measurements typically used Omega PX329 or PX429 transducers.

Low-speed temperature measurements were made in the acoustic cavities, injector manifolds, chamber and nozzle skin temperature, and various skin temperatures on the propellant lines. Hot-gas temperature measurements in the acoustic cavities were measured using type K exposed-tip probe thermocouples at various depths into the gas pocket of the acoustic cavity. Hot chamber and nozzle wall temperatures were measured using type K thermocouple wire welded into the chamber wall, creating an in-situ thermocouple. Injector manifold cryogenic temperatures were measured with type T exposed tip probe thermocouples. 2012 testing of the HD4 engine on vehicle 1.5a used grounded-tip thermocouples in the injector manifolds, but the response function was undesirably slow for startup transients. Exposed-tip thermocouples were subsequently used in all the vehicle 1.5b and SSC testing. Cryogenic skin temperature measurements were made with insulated thin film type T thermocouples.

Propellant flow rates were measured with turbine flowmeters of 1.5" or 2" diameter depending on test stand or vehicle operation. The flowmeters used included Turbines Inc model TMC-x-SAN and Hoffer model HO-x-CB-1M-TRI-X. The propellant manifolds in the SSC E-3 test stand downstream of the flowmeters were configured to mimic the vehicle propellant manifolds, shown in Figure 6, with some minor differences.

2. High-speed Instrumentation

High speed pressure measurements varied from the vehicle 1.5b configuration to the SSC test configuration. As the testing evolved, multiple layouts of the instrumentation were attempted, but the pressure transducer arrangement was always set to capture data with high-speed pressure transducers at 0 deg, 90 deg, and 135 deg orientation, shown in Figure 7.

High speed pressure measurement used two different types of transducers. Vehicle 1.5b testing used Omega DPX101, piezoelectric dynamic pressure transducers. In the SSC-E3 configuration, Stellar GT100 high-speed static transducers were used. In the SSC configuration, the Stellar transducers were often installed with long sense lines, sometimes as long as ˜5-8" in length due to sensor mounting configurations. Additionally, in some versions of the test evolution, the high-speed pressure sensors where mounted in the
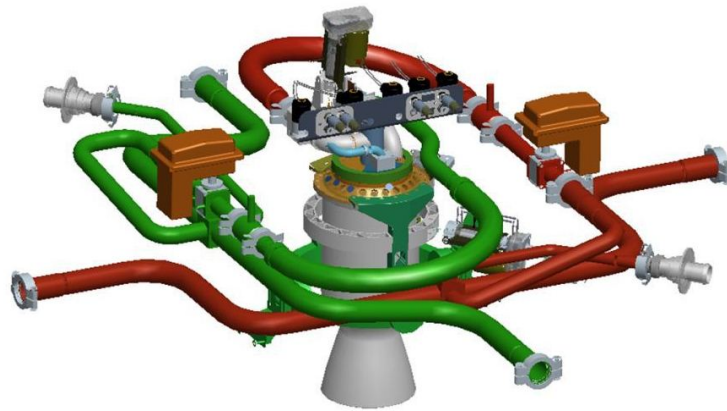
American Institute of Aeronautics and Astronautics

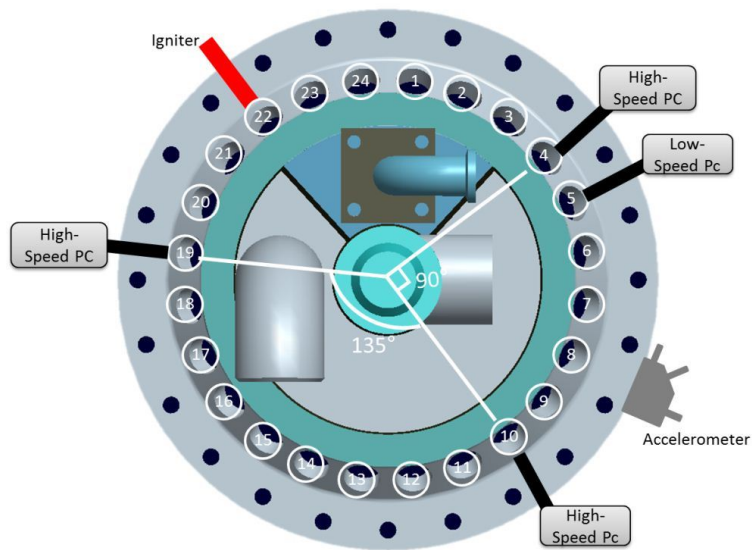**Figure 6. Morpheus main engine vehicle feedline configuration with flowmeters.**

Figure 7. Morpheus main engine high-speed instrumentation layout (top-down view). Typical layout shown, multiple layouts tested.

back of long acoustic cavities. Some testing was performed at SSC E-3 with Stellar and Omega piezoelectric transducers on the same or adjacent ports.

The accelerometers were mounted to the injector-chamber flange by a thick bolt-on steel plate. Two different makes of three-axis accelerometers were used during testing. For the vehicle tests, Endevco model 2221F accelerometers were used with the most success. For SSC-E3 testing, a Dytran model 3039C accelerometer was tested with the most success.

For vehicle tests, high speed instrumentation was recorded through with a HBM SoMat EDAQ Lite recorder, typically recording at 20 kHz. For SSC-E3 testing, data was recorded through the facility DataMAX DTX-9R recorder, typically at 25 kHz, with some short-duration tests recorded up to 102.4 kHz. Post-processing and spectral analysis of high-speed instrumentation was conducted in Matlab Signal Processing Toolbox.

D.   High Speed Redline System

The high speed combustion instability observed on the test stand typically manifested too quickly for manual test conductor intervention and initially caused significant yet repairable damage to the HD5 injector at SSC. To limit exposure to this ignition risk, an instability detection and automated engine shutdown system was added to the test stand and Morpheus flight avionics. This system utilized high speed chamber pressure data, and was initially created on-demand during a SSC HD5 test campaign, two days after the identification of the ignition stability issue.

Several iterations of the system were attempted, ranging from a reconfiguration of the existing SSC DataMAX outputs, to a simple voltage integrator, to the final system, which was a standalone analog circuit monitoring raw voltage from two of the DPX101 high speed piezoelectric sensors. This system sent the Morpheus flight computer an integrated, amplified, and smoothed voltage tailored to the 3-6 khz signal range (although any oscillatory signal would increase the output voltage). The flight computer treated these input voltages as a standard configurable redlines (two independent redline channels). The μsec response rate sensor and analog circuit provides nearly instantaneous indication of instability to the Morpheus flight computer. With persistence checks, the combined redline system and Morpheus flight computer was able to command an engine shutdown within ~40 ms from the onset of instability.

The high speed redline system was used for all engine hot-fire events on the test stand and Morpheus vehicle. The availability of real-time instability protection allowed for the exploration of the ignition instability issue and continuation of flight testing with substantially reduced risk of instability-related damage to the engine hardware, test stand, or vehicle.

III.   Results, Throttling and Chug Stability

The Morpheus main engines demonstrated low Pc throttling across a 4:1 throttling range. Chug instability was never observed during mainstage throttling in the vehicle tests or in SSC testing. However, chugging was observed during some engine shutdown sequences in the vehicle tests and SSC tests. Figure 8 shows an example pressure measurements and power spectral density (PSD) plot of a free-flight vehicle test demonstration that exhibited chug during shutdown. Additionally, chug was infrequently observed in during engine startup in some off-nominal SSC tests.

The main engines were designed to have injector pressure drop ΔP ratio, $\Delta P/Pc$, at ~25-32% at full thrust and ~9-11% at low throttle (4:1) for the various engine configurations. However, test results showed that the actual pressure drop at low throttle was actually higher than predicted, $\Delta P/Pc$ ~15%. The engine throttling is achieved by varying the main engine ball valve position at a constant tank and engine inlet pressure. Because the main engine ball valves were never operated full-open, the valves effectively throttled the propellants to a pressure that was limited by the by the vapor pressure of the propellant. This throttling effect from the valves provided a cushion pressure that prevented the injector from operating down to the low throttle design $\Delta P/Pc$, and may have prevented the onset of chug at very low power levels. In order to fully test the engine at the $\Delta P/Pc$ ~9-11% range, the engine would need to be purposely tested with the engine ball valves "wide-open" and lower tank operating pressures (testing not performed to date).
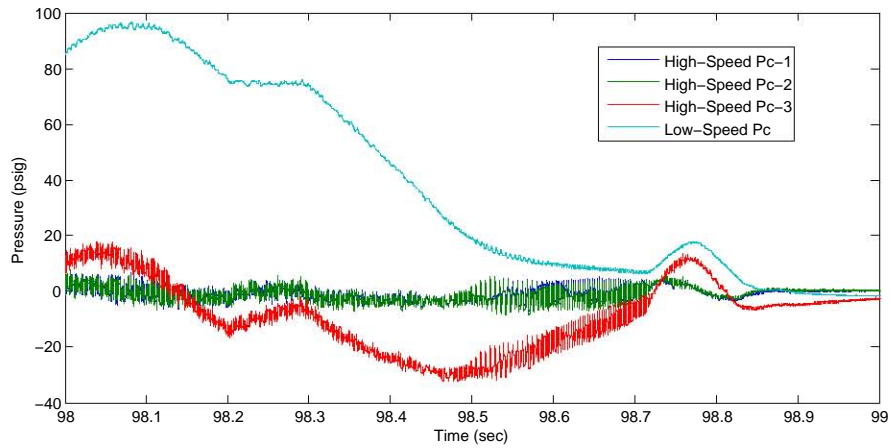
(a)
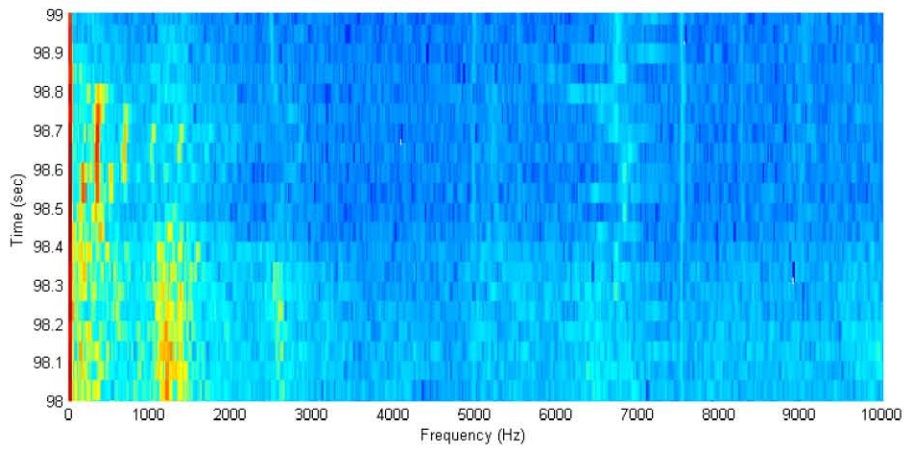
(b)

Figure 8. Free-flight 12 vehicle demonstration with HD4-A-LT, chug onset during main engine shutdown. (a) High-speed and low-speed pressure measurement during shutdown. (b) PSD of high-speed pressure measurement during shutdown. PSD units arbitrary.

American Institute of Aeronautics and Astronautics

A. Chug Stability in the Morpheus Vehicle Configuration

As mentioned above, chug was never observed during mainstage throttling during vehicle tests. Chugging was only observed on some tests during shutdown. The observed chug frequency on the Morpheus vehicle was ˜350 Hz. Shutdown chug was only observed during ground-based testing (e.g., hold-down hot-fire tests or tests with ground takeoff and landing), and chug was never observed in tether tests when the vehicle was suspended above the ground. For comparison, the engine nozzle exit in the Morpheus vehicle is less than two feet above the bottom of the vehicle feet. During landing, the engine shuts down with the nozzle exit less than 3 nozzle diameters off the ground; whereas during suspended tether tests, the whole vehicle may be 15 or more feet above the ground during "landing" and engine shutdown. Therefore, it is assumed that the chug was aggravated by ground-interaction acoustics, similar to the screech instabilities described later.

Using HD4-A-LT on Morpheus vehicle 1.5b, the maximum pressure observed for any onset of chugging on the vehicle during shutdown was ˜50 psig, just below the 4:1 low throttle setting, and the maximum $\Delta P/Pc$ for any onset of chugging on the vehicle during shutdown was ˜9-15% psid/psia. Most free-flight landing throttling included low throttle levels down to ˜80 psig prior to shutdown. In some tether and ground hold-down tests, the vehicle successfully throttled down to ˜60-75 psig, $\Delta P/Pc$ ˜14-17% psid/psia without chugging. Figure 9(a) shows a $\Delta P/Pc$ map for the oxygen and methane manifolds, indicating the relative limit for onset of the chug during engine shutdown in vehicle tests, and Figure 9(b) shows the chug range plotted for Pc. The 4:1 low-throttle demonstration points are also shown in Figure 9.

B. Chug Stability in SSC-E3 Configuration

Similar to the vehicle configuration, chugging was never observed during mainstage throttling in the SSC-E3 configuration. The shutdown chugging was observed for all three engines, HD4-A-LT, HD4-B-LT, and HD5. The observed chug frequency in the SSC-E3 test stand was ˜150-200 Hz. The lower frequency of the SSC-E3 configuration chugging compared to the vehicle configuration was due to the overall tank-feedsystem line lengths at SSC-E3 being much longer than the overall vehicle line lengths.

The maximum observed pressure of the shutdown chugging at SSC was slightly higher than the vehicle; chugging was observed in shutdown at pressures up to 65 psig, at $\Delta P/Pc$˜13-19% psid/psia maximum. The lowest mainstage throttle demonstrations in the SSC-E3 configuration were conducted on HD4-A-LT; Pc down to ˜70 psig was tested, and $\Delta P/Pc$ was tested as low as ˜8-17% psid/psia successfully without chug. The chug characterizations for $\Delta P/Pc$, Pc, and the low-throttle demonstrations for the SSC-E3 tests are shown in Figure 9.

Additionally, some early HD4-A-LT and HD5 off-nominal testing demonstrated chugging during the startup sequence under certain conditions. These startup-chug data points demonstrated the chug onset at low Pc, similar to the shutdown chug observation, shown in Figure 9(b). However, these startup chug cases occurred with much higher $\Delta P/Pc$, in the same range as the mainstage $\Delta P/Pc$, shown in Figure 9(a). These tests were conducted early in the SSC-E3 test campaigns with aggressively off-nominal startbox inlet conditions and sequences. In the subsequent tests of HD4-A-LT and HD4-B-LT with nominal startbox conditions and sequences, the startup chugging was not observed.

IV.   Results: High-Speed (Screech) Combustion Stability

During main engine development testing, the Morpheus main engines demonstrated high-speed (screech) acoustic-coupled combustion instabilities. The instabilities were never observed to initiate during mainstage operations. The instabilities typically initiated during engine startup. At SSC, for example, the instabilities triggered almost immediately following the methane injector fill indicated by the fuel manifold thermocouple. If the engine was subsequently throttled up from the startup power level to mainstage, the instability would almost always decay at the throttle-up transition. However, tests at SSC-E3 did demonstrate the capability of the screech instability to propagate into mainstage. Figure 10 shows an example of a SSC-E3 test with HD4-A-LT with a combustion instability that decayed at throttle-up, and Figure 11 shows an example of test where the instability propagated into mainstage on HD5.

As measured on the close-coupled piezoelectric dynamic pressure transducers, the instabilities could typically reach amplitudes up to ˜35-45% psid/psia (peak-to-peak). The highest amplitude measured during a test was ˜50-80% psid/psia. Note that data recorded in the SSC-E3 configuration using the static transducers often showed amplitudes much higher, as shown in Figures 10(a) and 11(a). However, it is believed that the
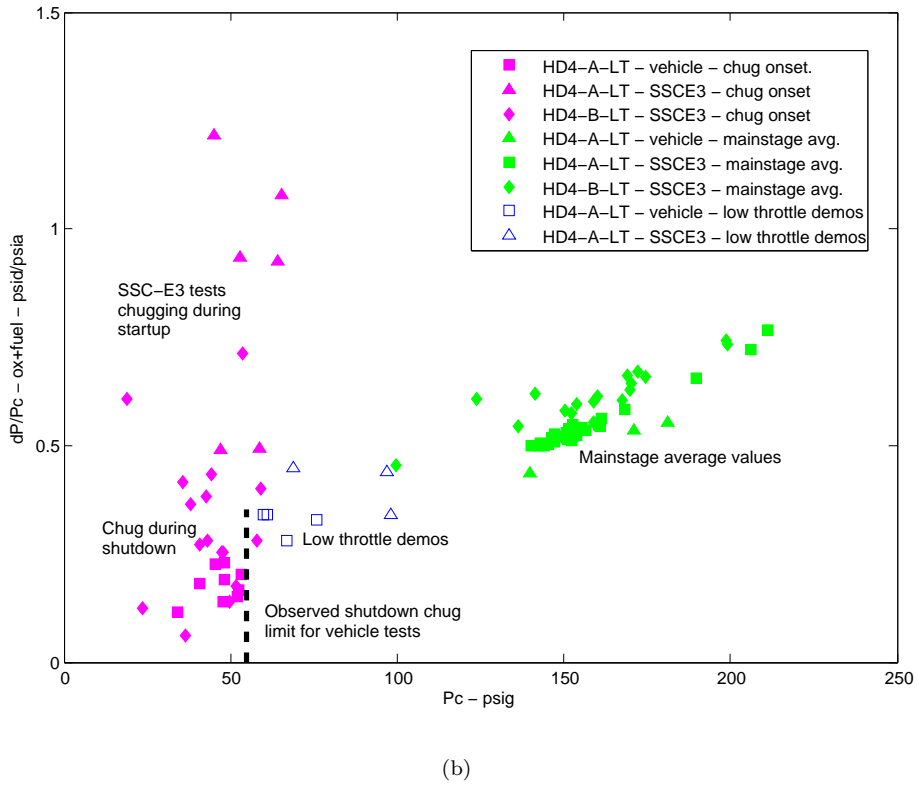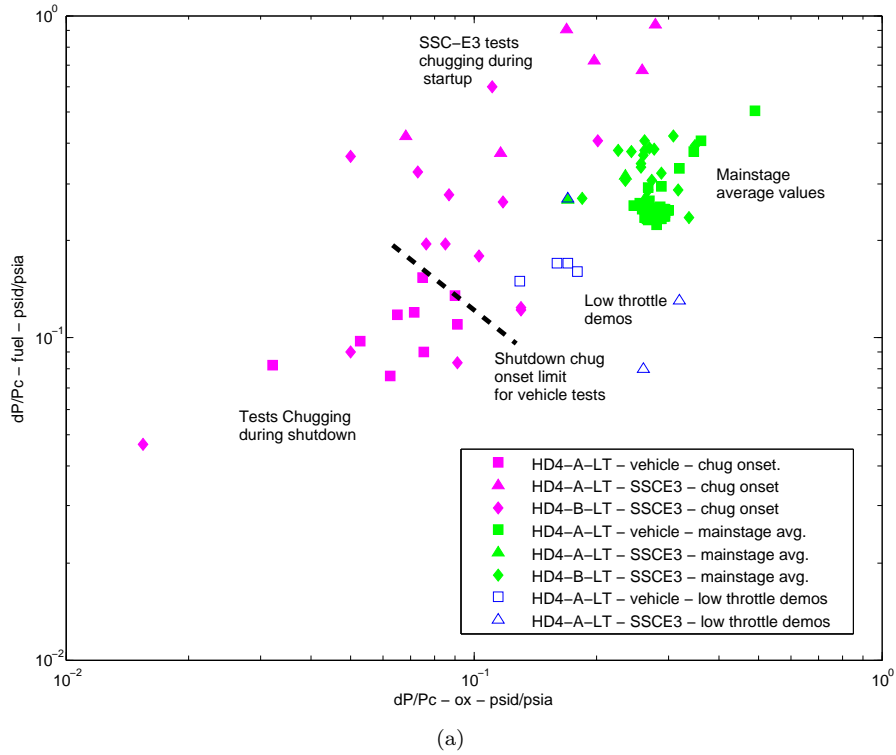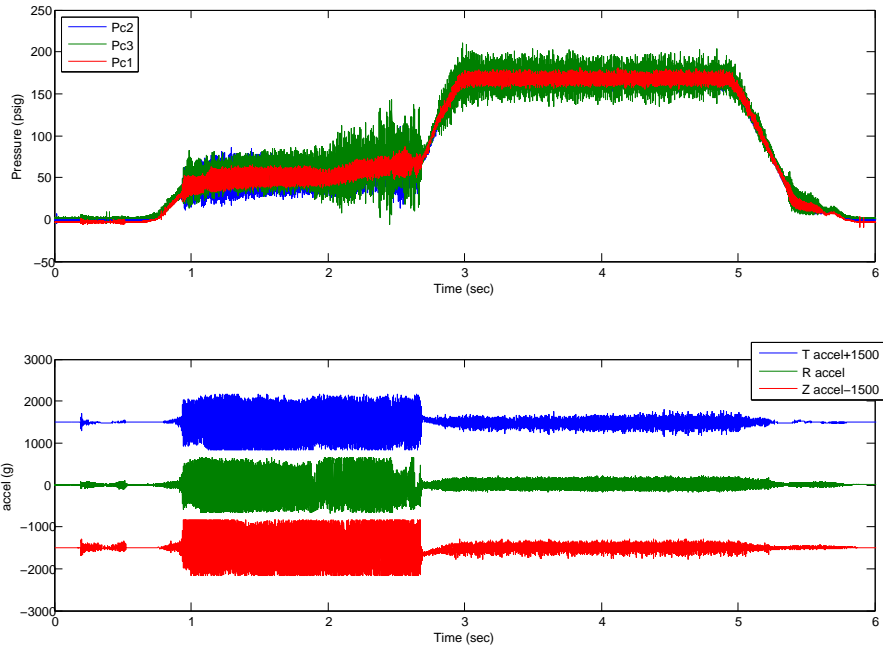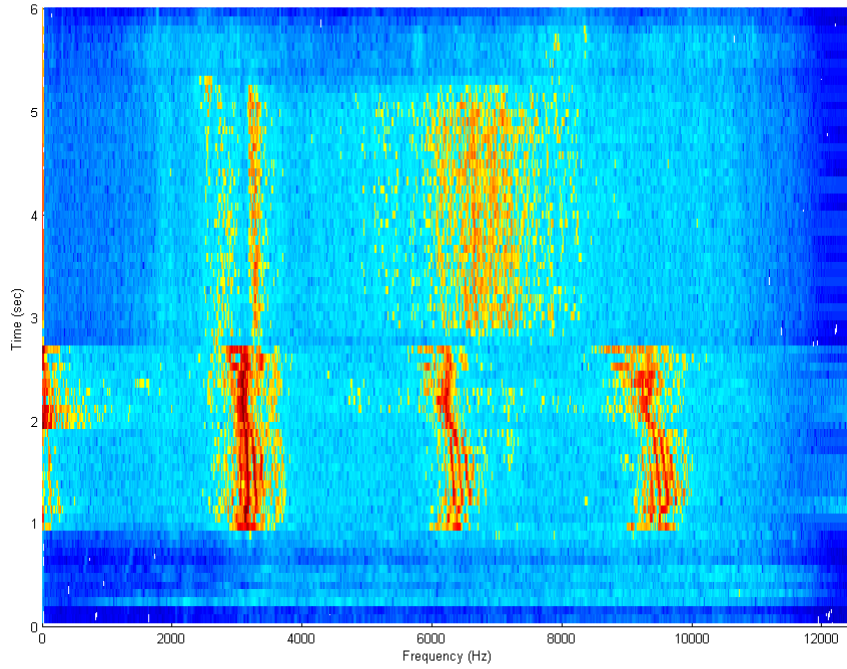
(a)

(b)

Figure 9. HD4-A-LT and HD4-B-LT Chug characterization, vehicle and SSC-E3 tests shown. (a) $\Delta P/Pc$ for oxygen and methane manifolds. (b) $\Delta P/Pc$ (LOX + methane) and Pc.

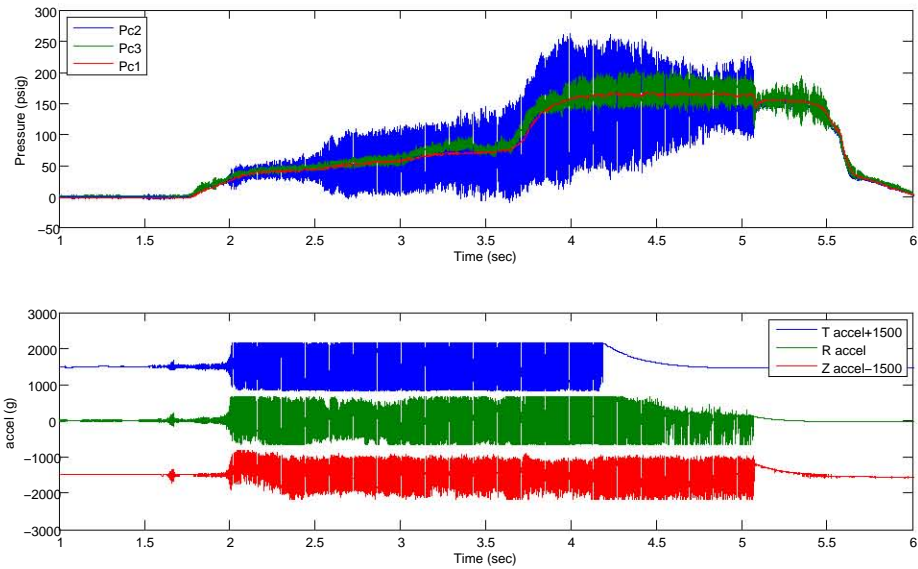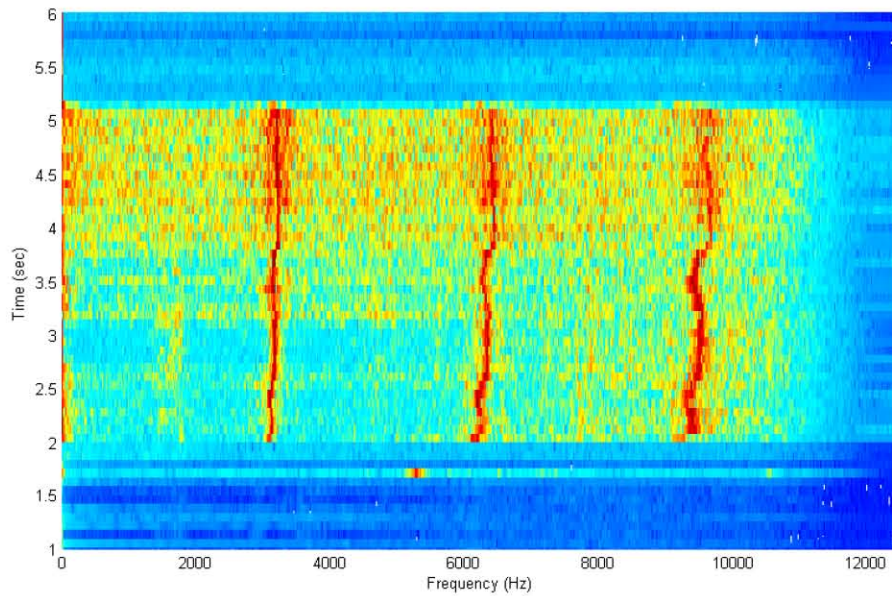American Institute of Aeronautics and Astronautics

(a)

(b)

Figure 10. High-speed (screech) combustion instability during SSC-E3 test 14 of HD4-A-LT. Instability decays at throttle-up. (a) High-speed *Pc* and accelerometers. (b) PSD of accelerometer, sampling rate 25 kHz. PSD color scale arbitrary.

American Institute of Aeronautics and Astronautics

(a)

(b)

Figure 11. High-speed (screech) combustion instability during SSC-E3 test 10 of HD5. Instability propagates into mainstage. (a) High-speed *Pc* and accelerometers. (b) PSD of accelerometer, sampling rate 25 kHz. PSD color scale arbitrary.

.

SSC-E3 static transducer amplitudes were affected by sense line length, and the close-coupled piezoelectric dynamic transducers used on the vehicle testing more accurately measured the instability amplitude.

The instabilities were observed in the HD4-A-LT and HD5 engine configurations. Table 1 shows the number of tests with screech instability for the different engine configurations on the vehicle and at SSC-E3. The PSD in Figure 10(b) shows distinct tones at 3125 Hz, 6250 Hz, and 9400 Hz. This 3-6-9 kHz pattern is characteristic of both the HD4-A-LT and HD5 screech instabilities (similar in Figures 10(b) and 11(b)), and is believed to be 1T, 1R, and 1T1R, as discussed in the next section.

A.   Test Observation History

1.   Early Development Tests

Prior to the 2012 vehicle testing with HD4-A (small throat baseline), early Morpheus development testing in 2011-2012 was performed with the HD3 main engine. HD3 had demonstrated no instability problems until a suspected 1T-related burn-through during a vehicle test (triggered at ignition). The 1T instability was suspected to be related to an over-chilled LCH4 condition, which would later re-emerge during HD4-A-LT and HD5 testing. After the HD3 burn-through, HD4 design modifications included a re-design of the acoustic cavity ring orientation.

In 2012, HD4-A (small throat baseline) was tested 19 times on Morpheus vehicle 1.5a with no detected instability problems. Some instances of a 1T acoustic tone were present during some engine startups, but these transient tones were low-amplitude and momentary.

2.   SSC-E3 Test Observations

Following the Morpheus vehicle 1.5a crash in 2012, engine testing resumed later in 2012 at SSC-E3 with the HD5 engine. HD5 testing revealed significant combustion instability issues (1T, 1R, 1T1R, etc.), and subsequent SSC-E3 testing of HD4-A-LT revealed the same significant combustion instability problems were present in both engine configurations.

Data analysis from the SSC-E3 tests with combustion instability indicated two major drivers. First, over-chilled LCH4 inlet conditions typically caused the worst instabilities (1T, 1R, 1T1R, etc.) at engine start, and HD5 tests showed this instability could propagate into mainstage. Figures 10 and 11 show examples of instabilities resulting from over-chilled LCH4. Second, lower-amplitude combustion instabilities could be triggered by "warm LOX" inlet conditions. The "warm LOX" instabilities appeared as 1T-1L modes or 1R modes and dampened out once the LOX injector chilled in. Figure 12 is an example of a test with two different screech instability mechanisms during a single test. The initial instability occurs due to "warm LOX", resulting in a 1R-only mode that dampened out as soon as the LOX injector chilled in, and the second instability due to "cold methane" resulting in the more severe 1T-1R-1T1R-etc mode when the fuel injector chilled in.

By the time HD4-B-LT was tested at SSC in 2013-2014, the major operational controls for the combustion instability had been employed, and no screech instabilities were observed on HD4-B-LT at SSC-E3. These controls included increasing the engine start-up to approximately 50% power level and maintaining proper propellant conditioning (very cold oxygen inlet with room temperature methane inlet).

3.   Morpheus Vehicle Test Observations

When the vehicle 1.5b build-up was completed in 2013, testing started with the HD4-A-LT main engine. Vehicle testing with HD4-A-LT also demonstrated major combustion instability issues similar to the observations from the SSC-E3 testing. Data analysis showed that the instability was worsened by propellant inlet startbox conditions and low Pc engine startup conditions. In some short duration, off-nominal startbox testing on the vehicle, the instability could even initiate during engine shutdown.

Successful vehicle test demonstrations were achieved by altering the main engine startbox conditions to enforce a "cold LOX", "warm methane" start condition. The engine start sequence was also modified to allow a higher Pc engine startup that would still meet Morpheus vehicle requirements. As discussed earlier, the Morpheus vehicle transitions through a low-g idle state prior to liftoff, so the main engine must be started at a low Pc to prevent premature liftoff. This low Pc startup had significant impacts to the main engine combustion stability.
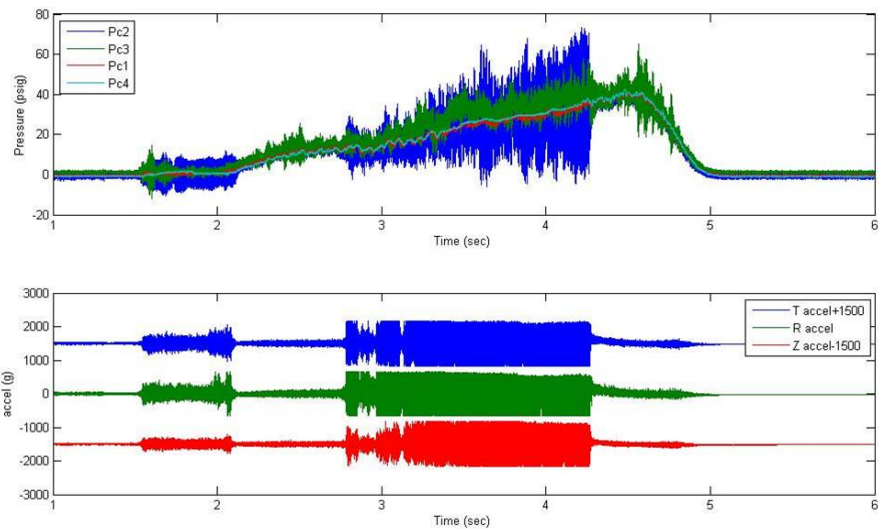
(a)
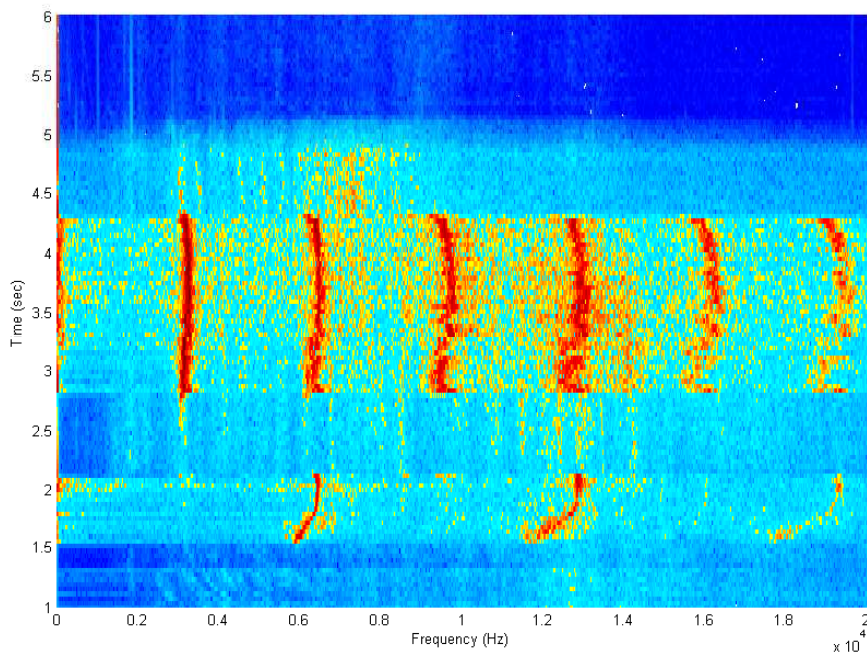
(b)

Figure 12. High-speed (screech) combustion instability during SSC-E3 test 6 of HD5. Two different screech instability mechanisms during a single test. The initial instability (1.5-2 sec) occurs due to "warm LOX" resulting in a 1R-only mode that decayed when the LOX injector chilled in, and the second instability (3-4 sec) due to "cold methane" resulting in the 1T-1R-1T1R-etc mode. (a) High-speed Pc and accelerometers. (b) PSD of accelerometer, sampling rate 102.4 kHz. PSD color scale arbitrary.

Compared to HD4-A (small throat baseline), the "large throat" HD4-A-LT injector pressurization and injection velocity profile is higher (i.e., the larger throat affects chamber pressurization and injector pressure drop). As shown later, the screech instability is theorized to be the result of excessive injection velocity at low Pc, which explains why major combustion instabilities were not observed with vehicle 1.5a using HD4-A (small-throat baseline).

Similar to the chug instability issue, the vehicle test screech combustion instability appeared to be aggravated by ground interaction acoustics. Combustion instability was only observed during tests that were close-coupled to the ground (e.g., ground hold-down tests, ground-based takeoff and landing tests). In these ground-based tests, mechanical ringing of the main engine bell could be seen on the accelerometers post-shutdown, even in some tests that did not trigger combustion instability. Figure 13 shows an PSD of an accelerometer channel from an unstable test on the vehicle during a hold-down hot-fire demonstration. Mechanical ringing can be seen post-engine shutdown at 490 Hz, 1,000 Hz, 1,800 Hz, and 2,850 Hz. Tap tests on the engine bell demonstrated mechanical ringing at 480 Hz, 1,000 Hz, 1,500 Hz, and 1,880 Hz.
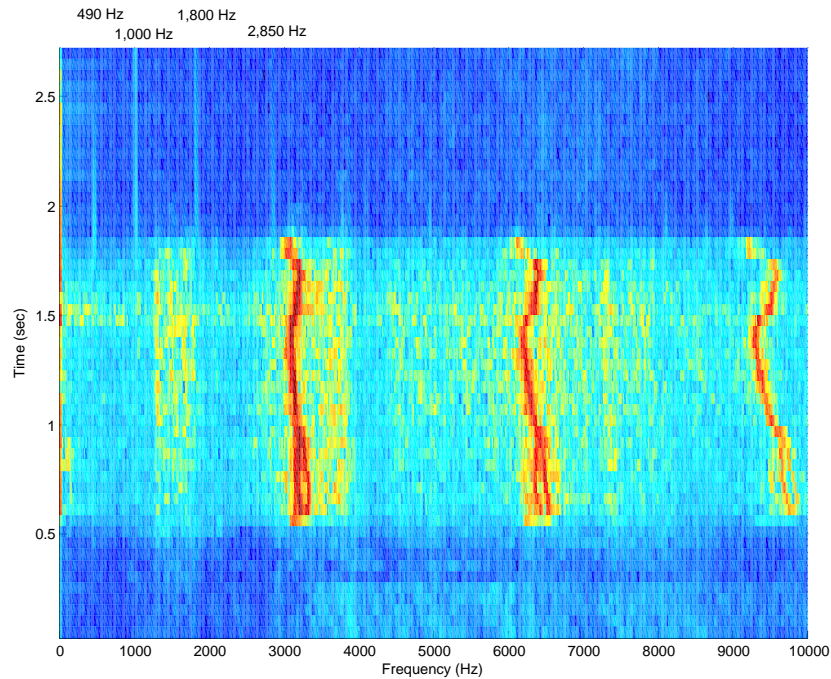

Figure 13. Accelerometer PSD of hot-fire test 9.1 from the Morpheus vehicle 1.5b using HD4-A-LT with combustion instability. Note mechanical ringing of the engine bell post-shutdown at 490 Hz, 1,000 Hz, 1,800 Hz, and 2,850 Hz. Sampling rate 20 kHz. PSD color scale arbitrary.

B. High-Speed Waveform Analysis

As evident in every combustion instability test, the root tone of the instability appeared approximately 3,125-3,250 Hz average. Table 2 shows the predicted and measured acoustic modes of the chamber. For the predictions, chamber length was assumed to be face to throat, chamber diameter was assumed to be head-end diameter (large than face diameter). Chamber sound speed was assumed to be 3,600 ft/sec, based on previous work and HD4 engine performance modeling using a degraded characteristic velocity, C^*, factor. The measured 3,125 Hz root tone appears to match the predicted 1T mode. Figure 14 shows Morpheus vehicle hot-fire test 9.1 of HD4-A-LT with a combustion instability (the same test as shown in Figure 13). In Figure 14, the close-coupled dynamic piezoelectric transducers Pc-1 and Pc-2 are mounted circumferentially 135 deg apart. The resultant data is 180 deg out of phase at ~3,300 Hz. Therefore, this out-of-phase signal is interpreted as a standing 1T mode.

As mentioned above, the characteristic signature of the high-speed (screech) combustion instability was a pattern of 3,125 Hz, 6,250 Hz, and 9,400 Hz (average values). This 3-6-9 kHz integer pattern persisted regardless of high-speed data acquisition rate, and appeared in waveform by inspection and by PSD plots.

American Institute of Aeronautics and Astronautics

Table 2. Approximate Morpheus main engine HD4-A-LT chamber acoustics (note that HD5 predictions/measurements slightly different). Predicted values at 3,600 ft/sec chamber sound speed.

Mode	Predicted (Hz)	Measured (Hz)
1L	1,440	1,460
2L	2,890	2,930
3L	4,330	4,400
4L	5,770	5,880
1T	3,150	3,125
2T	5,200	-
3T	7,200	-
1R	6,550	6,250
2R	12,000	-
3R	17,400	-
1T1R	9,100	9,400
1T2R	15,000	-
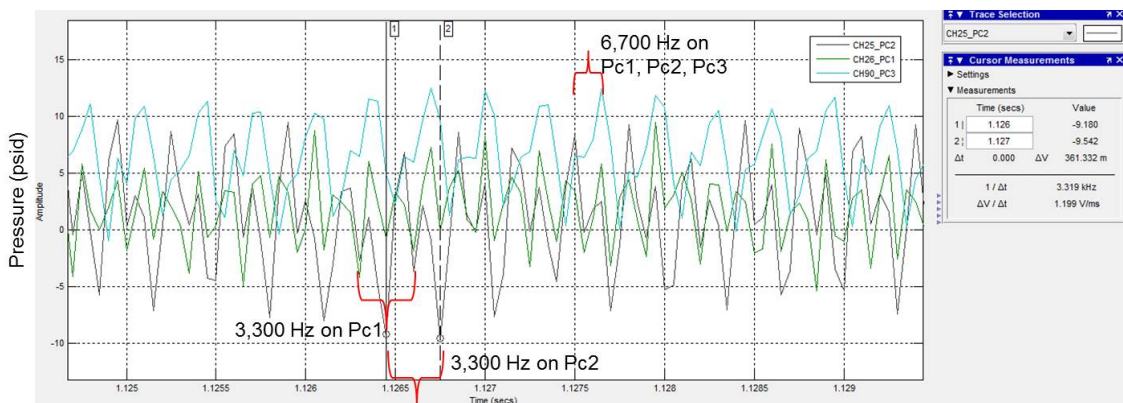
Figure 14. High-speed pressure measurement from HD4-A-LT vehicle hot-fire test 9.1 with combustion instability (same test shown in Figure 13). Sampling rate 20 kHz, close-coupled dynamic piezoelectric transducers used. *Pc-1* **and** *Pc-2* **are mounted circumferentially 135 deg apart, and measured signals are 180 deg out of phase at 3,300 Hz, assumed to be 1T mode.** *Pc-1*, *Pc-2*, **and** *Pc-3* **are in phase at 6,700 Hz, assumed to be 1R mode.**

American Institute of Aeronautics and Astronautics

As shown in Table 2, the higher order tangential modes (2T, 3T) are not observed in the data. Therefore, determining the correct acoustic-coupled mode is not straightforward by inspection alone.

Figure 14 shows all three dynamic piezoelectric dynamic pressure transducers from Morpheus vehicle hot-fire test 9.1 with HD4-A-LT. *Pc-1*, *Pc-2*, and *Pc-3* are in phase at ~6,700 Hz. Given the phase agreement of the pressure transducers at ~6,700 Hz and the close approximation to the predicted acoustic frequency, the tone is assumed to be a 1R. In this case, the tone has been frequency-modulated from the predicted value (6,550 Hz) to a value that is an integer multiple of the 1T mode. The average value of the measured 1R tones was ~6,250 Hz for most tests. If the ~6,250 Hz had been a 2T or 3T, it would have required even further frequency modulation from the predicted values of 5,200 Hz or 7,200 Hz, respectively (see Table 2).

Further evidence of the 1R acoustic mode was recorded in HD5 test 6 at SSC-E3, which was recorded at 102.4 kHz high-speed instrumentation. As shown in Figure 12(b), the initial "warm LOX" instability had a different signature than the later "cold methane" instability. The initial instability contained no waveform at 1T (~3,200 Hz), but it did exhibit a 1R mode at ~6,450 Hz with harmonics. The second instability did contain the more typical pattern of 1T, 1R, 1T1R with tones at 3,160 Hz, 6,520 Hz, and 9,640 Hz. Figure 15 shows the accelerometer waveform, which indicates the frequency content. At the 102.4 kHz sampling rate, higher order harmonics appear: 2R at ~12,900 Hz, 1T2R at ~16,200 Hz, and 3R at ~19,000 Hz. Frequencies at 1T3R (~20,000 Hz and above) appear in the PSD calculation, but are not distinguishable in the measured waveform.
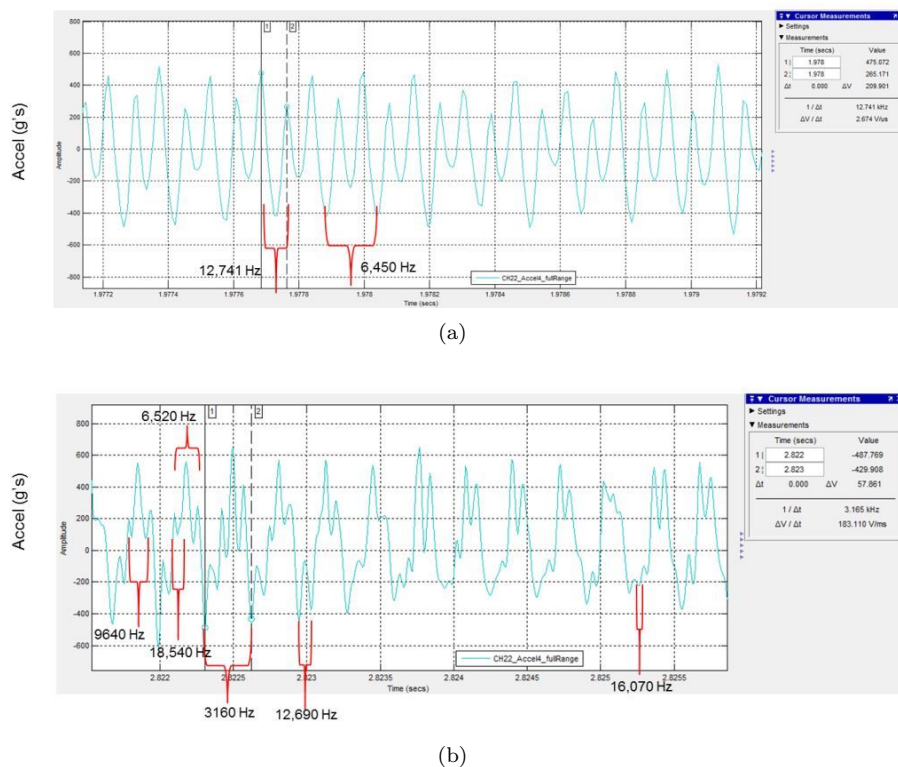

(a)

(b)

Figure 15. High-speed accelerometer measurement from HD5 test 6 at SSC-E3 with combustion instability (the same test 6 as shown in Figure 12). Sampling rate 102.4 kHz. (a) Initial "warm LOX" instability with 1R at 6,450 Hz plus 2R harmonic. (b) Subsequent "cold methane" instability with 1T at 3,160 Hz, 1R at 6,520 Hz, 1T1R at 9,640 Hz, and R-harmonics up to ~19,000 Hz.

There is support in available literature for an acoustic mode of 1R at exactly 2 times the 1T frequency. Yang et al. developed an acoustic model that demonstrated that non-linear coupling can modulate both the 1R and 2T to oscillate at exactly twice the 1T frequency.[6] In their analysis, the 1R coupling was higher amplitude because of energy transfer from the 1T to the 1R.

The non-ideal high-speed pressure transducer layout complicated determination of the acoustic modes. In many of the SSC-E3 tests, transducers were mounted on the back end of acoustic cavities or were installed with relatively long sense lines. This pressure transducer arrangement made interpretation of the phasing of the signals complicated. For example, in some tests, one of the high speed *Pc* transducers could read a large

American Institute of Aeronautics and Astronautics

amplitude event only on one channel, or there could be significant variable phasing between the Pc channels. As shown in Figures 10(a), 11(a), and 12(a), the separate Pc signals often exhibited different amplitude signals or characteristics. In addition to the transducer installation issues, there was also significant noise in the data acquisition system at ~6,000-6,500 Hz that interfered with the measurement interpretation.

Since the characteristic instability acoustic pattern (3 kHz - 6 kHz - 9 kHz) appeared as integer-multiples, alternate theories were proposed to explain the signature. It was postulated that the distinct harmonic appearance of the PSD was the result of a sharp-fronted wave making a 1T mode appear to have integer harmonics. However, this conclusion is not supported given the waveform content apparent in both the 25 kHz and the 100 kHz sampling rate tests or the standalone 1R content observed without a 1T component (e.g., Figure 15).

Another proposed solution is that the apparent integer-harmonics are caused by L-modes. In this explanation, the ~3,100-3,200 Hz tones would be explained as 2L modes, and the ~6,200-6,700 Hz tones would be 4L. Although this idea provides a simplified explanation to the integer-harmonics, it would require significant frequency modulation for the L-modes (see Table 2). A different method of calculation the L-mode based on chamber length to the 2/3rd's of the nozzle entrance results in 1L at ~1,620 Hz, 2L at ~3,240 Hz, and 4L at ~6,490 Hz, and would require less frequency modulation. This estimation of the L modes is not clearly more accurate; some tests distinctly showed a 1L at ~1,460 Hz with the 2L, 3L, 4L harmonics as predicted (see Figure 16). Some tests did show a broader 1L pattern smeared out from ~1,400-1,700Hz, but the tones were not distinct in the PSD. The L-mode explanation also does not as easily explain the "warm LOX" instability observation in Figure 12, which would require a 4L mode as the root tone, without 1L or 2L being present. The preponderance of the evidence suggests that the 3 kHz - 6 kHz - 9 kHz pattern is not the L modes, but definitive test of the L-mode postulation would require a test campaign with a different length chamber (not performed to date).

C.   Operational Engine Controls for Combustion Stability

Data analysis revealed features common to the tests with combustion instabilities. All the instabilities occurred at low Pc with high injector $\Delta P/Pc$ during engine start, shown in Figure 17 for HD4-A-LT and HD4-B-LT. None of the instabilities observed on HD4-A-LT initiated once the injector was above ~50 psig during the startup sequence. As discussed in a previous section, the Morpheus vehicle required a low-g condition prior to liftoff, forcing the main engine to ignite into a low Pc condition. During this long startup time, the injector lingered at a high injector $\Delta P/Pc$ condition caused by the transient injector fill process. As shown in the next section, it is postulated that the high $\Delta P/Pc$ early in the injector fill process is the root cause of the combustion instability. Even in tests that were demonstrated stable, a momentary low-amplitude transient 1T (3 kHz tone only) mode would appear and decay in less than ~60-100 msec in many tests during the initial chill-in of the injector. The transient 1T tones had amplitudes <10% psid/psia (peak-to-peak) measured on the piezoelectric dynamic pressure transducers, typically ~4-7% psid/psia or less. Recall that the large amplitude instabilities were recorded at ~35-45% psid/psia.

As discussed previously, two operational controls were implemented to alleviate the high $\Delta P/Pc$ at low Pc condition. First, the startup sequence was optimized to the highest start Pc condition that still met the vehicle preflight hold-down force requirement. Secondly, a tighter operational control on "cold LOX" and "warm methane" startbox was maintained. Figure 18 shows the propellant inlet skin temperatures pre-start for HD4-A-LT and HD4-B-LT and the resultant stability trends. The propellant temperature startbox served to create an artificial LOX lead in the engine start sequence, enabling the engine start at higher Pc and higher mixture ratio. It should be noted that the startbox conditions also alleviated the trends of instabilities observed in SSC-E3 testing, where both the "warm LOX" and "cold methane" conditions could create instabilities.

V.   Injection Velocity Data Analysis

The root cause of the high-speed screech combustion instabilities is postulated to be an injection-coupled mechanism. The high $\Delta P/Pc$ at low Pc problem is symptomatic of orifice hydraulic flip phenomena and high injection velocity.
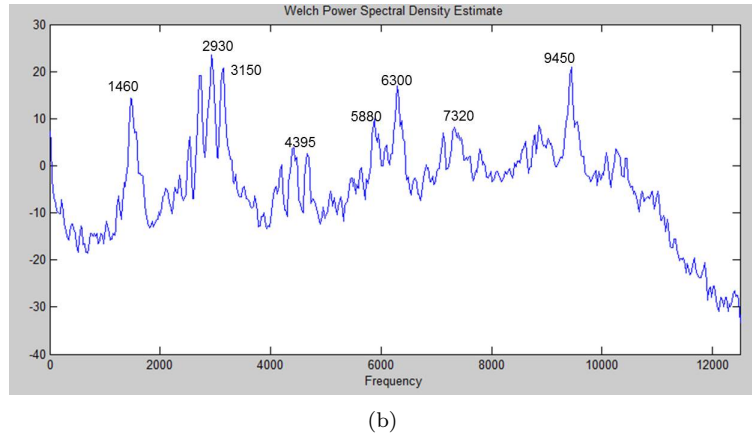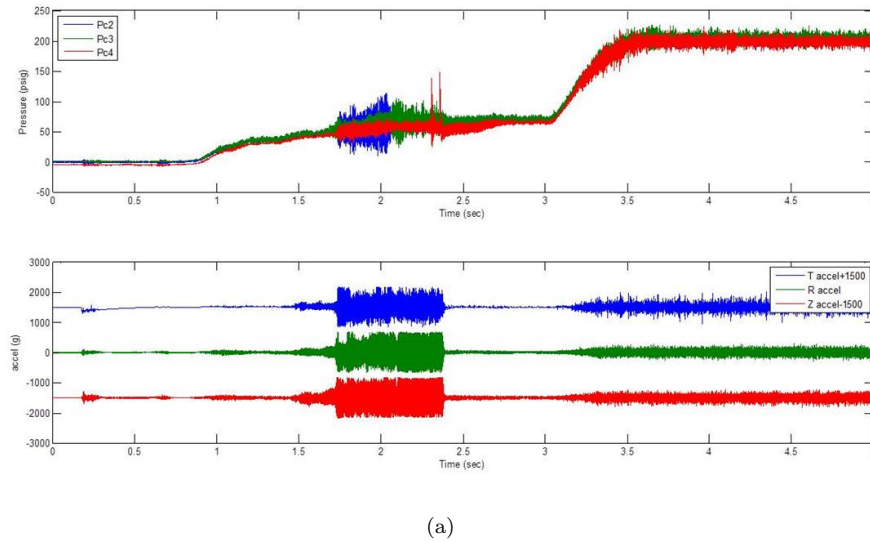
Figure 16. High-speed measurements from HD4-A-LT test 19 at SSC-E3 with 1L instability coincident with 1T-1R instability. (a) High-speed pressure and accelerometer data. (b) PSD of accelerometer, Sampling rate 25 kHz. PSD scale arbitrary.

A. Orifice Flow and Hydraulic Flip

Hydraulic flip in the injector orifices can be created at high $\Delta P/Pc$ at low Pc, and has been linked to combustion instability problems historically (see discussion in NASA SP-194[7] and NASA SP-8089[8]). In this operational condition, the injector orifice discharge coefficient, C_d, is abruptly shifted low, with flow separation (unattached) from the vena contracta. The problem creates high injection velocity and unstable flow patterns. The problem is worsened by the cryogenic propellants during injector chill-in since sub-cooling is minimal during the chill-in process, leading to low vapor pressure margin. The Apollo Service Propulsion System engine injectors were studied for hydraulic flip related to combustion instabilities, and C_d was found to jump from ~0.8 for full flow down to ~0.6-0.7 for hydraulic flip in water flow testing.[9] More recently, Nurick et al also studied water-flow hydraulic flip and cavitation in orifices, and found similar changes in C_d, with hydraulic flip occurring at low margin above vapor pressure.[10]

In order to investigate a possible phenomenological explanation for the observed instabilities in the Morpheus main engines, calculations for injection velocity, v, and C_d were performed using the measured low-speed engine data: injector face pressure drop (injector manifold - chamber pressure), ΔP, propellant flow-rate using the turbine flow meter, Q, and propellant density, ρ. Propellant density for the liquid propellant was calculated based on the measured injector pressure and temperature, either sub-cooled or saturated liquid. Note that using the measured value of flow-rate from the turbine flowmeter, Q, is clearly not ideal in the analysis since the primary area of interest is the startup transient.
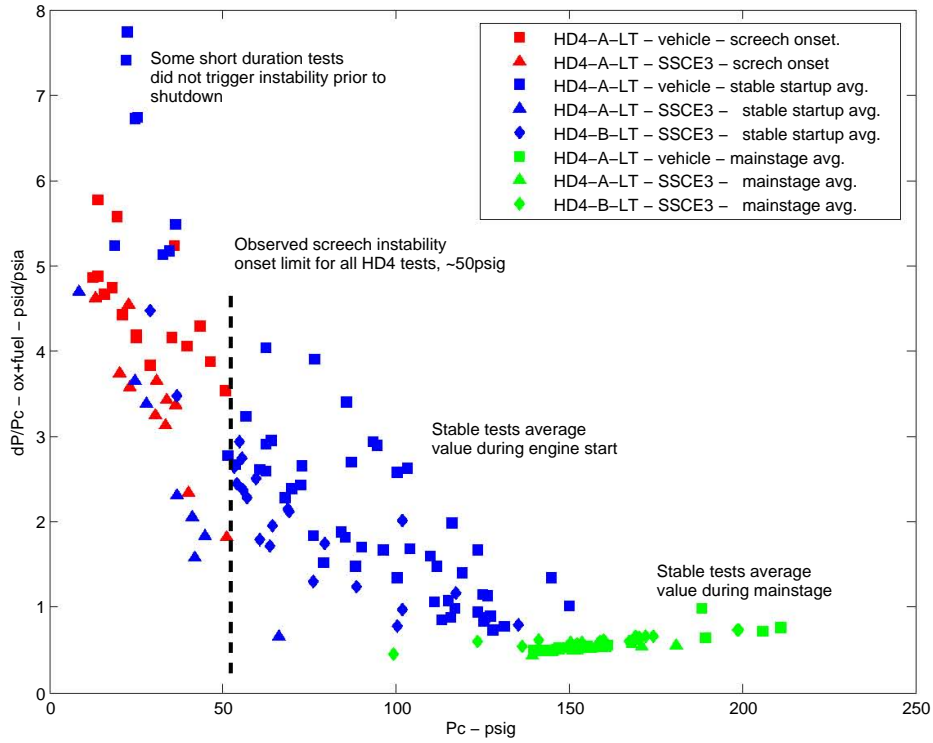
American Institute of Aeronautics and Astronautics

Figure 17. Combustion stability characterization of HD4-A-LT and HD4-B-LT for $\Delta P/Pc$ (ox + fuel) as a function of Pc. Note that all combustion instabilities onset at at high $\Delta P/Pc$ and Pc less than ~50 psig.
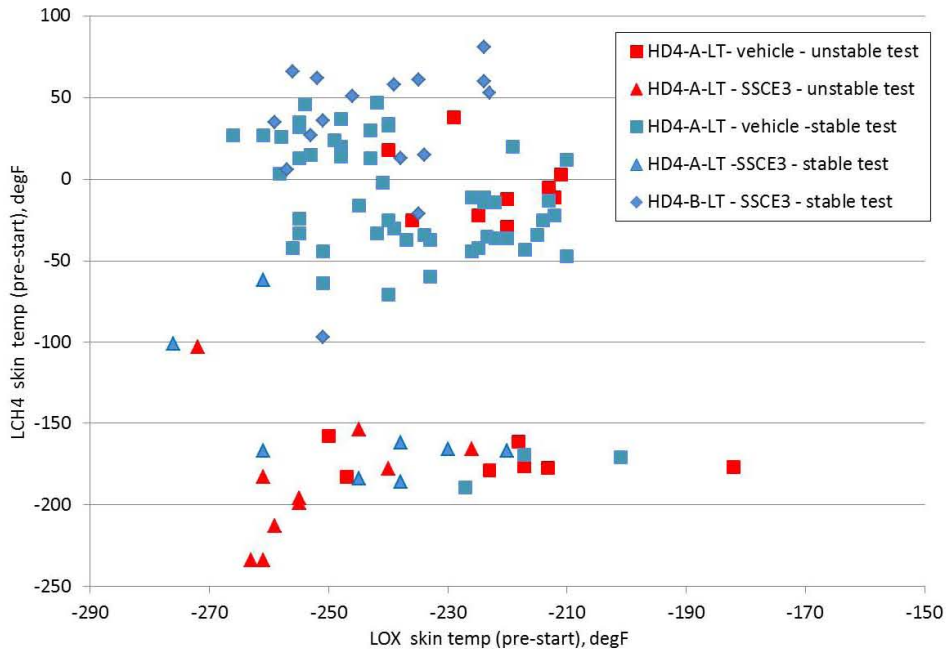

Figure 18. Combustion stability characterization of HD4-A-LT and HD4-B-LT for propellant inlet skin temperatures, pre-start, measured at the propellant flowmeters. Note best combustion stability controlled using "cold LOX" and "warm methane".

American Institute of Aeronautics and Astronautics

As shown in Equation 1, injection velocity is based on the Bernouli equation. Equation 2 calculates the injector orifice C_d based on total injector face orifice area, A, for each propellant.

$$v = \sqrt{2\frac{\Delta P}{\rho}} \tag{1}$$

$$C_d = \frac{Q}{vA} \tag{2}$$

The resultant data analysis for C_d using Equations 1 and 2 provided no clear indication of hydraulic flip in the value of C_d for either the LOX or the LCH4 injector orifices. No clear abrupt change in C_d was discernable as a result of ΔP during the injector transient chill-in process. In fact, the calculated startup transient Cd varied to significantly low values that were not physically realistic. In addition to the error introduced by using the transient turbine flowmeter data, this approach is also complicated by the two-phase density of the flow during the injector chill in process for the cryogenic propellants. Using a single-phase liquid density, ρ, in Equation 1 effectively masks any hydraulic flip because of variation in ρ due to the two-phase flow. In either event, the hydraulic flip or reduced propellant density has the same effect of lowering Cd.

B.   Two-Phase Injection Velocity Approximation, Hewitt Stability

As reported by several authors (e.g., Anderson et al,[11] Hulka and Hutt,[12] and Muss[13]), combustion instability in impinging-element liquid rocket engines has been characterized by key parameter, d/v, originally identified by Hewitt. The characteristic d/v relates a propellant orifice diameter, d, to the injection velocity, v. As described by Anderson at al, d/v is characteristic of the jet atomization frequency.[11]

An initial calculation approach was attempted using the liquid-phase density, ρ, and Equation 1 to calculate injection velocity, v. However, the results showed no distinct differences in v between the test demonstrations with and without combustion instabilities. As was noted in the C_d calculation analysis above, it was determined that the single-phase liquid density, ρ, was not realistically approximating the injected propellant conditions during the startup transient when the instabilities were triggering.

1.   Two-Phase Density Calculation

In the pursuit of an injection velocity calculation that could be used in a Hewitt d/v assessment, a two-phase orifice flow calculation was performed. Using either the homogeneous model or Chisholm models described in Reference 14, the two-phase quality, x, of a fluid can be calculated assuming a known total mass flow rate, $\dot{m}$, constant C_d, two-phase pressure drop, $\Delta P_{2\phi}$, and saturated liquid and gas phase densities, ρ_l and ρ_g. Quality is defined so that $x = 0$ at saturated liquid and $x = 1$ at saturated vapor. Both the homogenous model and the more accurate Chisholm model were calculated, and overall results were similar.

As described in Reference 14, The Chisolm model allows slip between the phases, and the liquid phase, vapor phase, and two-phase pressure drops are separated. The liquid phase pressure drop, ΔP_l, is defined in Equation 3, and the relationship between the between ΔP_l and $\Delta P_{2\phi}$ is defined in Equation 4.

$$\Delta P_l = \frac{\dot{m}^2(1-x)^2}{2\rho_l(C_dA)^2} \tag{3}$$

$$\frac{\Delta P_{2\phi}}{\Delta P_l} = 1 + \frac{C}{X} + \frac{1}{X^2} \tag{4}$$

The Lockhart-Martinelli constant, X, is defined in Equation 5. The Chisholm empirical constants, C and K, are defined in Equations 6 and 7.

$$X = \left(\frac{1-x}{x}\right)\left(\frac{\rho_g}{\rho_l}\right)^{0.5} \tag{5}$$

$$C = K\left(\frac{\rho_g}{\rho_l}\right)^{0.5} + \frac{1}{K}\left(\frac{\rho_l}{\rho_g}\right)^{0.5} \tag{6}$$

American Institute of Aeronautics and Astronautics

$$X < 1 \qquad K = \left(\frac{\rho_l}{\rho_g}\right)^{0.25}$$
$$X \geq 1 \quad K = \left(\frac{\rho_l}{\bar{\rho}}\right)^{0.5} = \left(1 + x\left(\frac{\rho_l}{\rho_g} - 1\right)\right)^{0.5} \tag{7}$$

Equations 3 and 4 are combined into Equation 8 for the total $\dot{m}$.

$$\dot{m} = C_d A \left(\frac{1}{1-x}\right) \sqrt{2\rho_l \Delta P_{2\phi} \left(1 + \frac{C}{X} + \frac{1}{X^2}\right)^{-1}} \tag{8}$$

Equation 8 was solved for each data point to calculate propellant two-phase quality, x. The total $\dot{m}$ was calculated from the measured turbine flowmeter flow rate, Q, and liquid density, ρ_l, was assumed at the flowmeter (upstream of the injector) based on injector manifold temperatures and pressures. The discharge coefficient, C_d, was assumed constant at the value calculated with Equation 2 for the injector mainstage average. Lastly, two-phase density was calculated from the quality, as shown in Equation 9. In these calculations, ρ_l is allowed to be sub-cooled if the propellant temperature is less than the saturation temperature.

$$\rho_{2\phi} = x\rho_g + (1-x)\rho_l \tag{9}$$

The calculation results for the two-phase density, $\rho_{2\phi}$, are shown in Figure 19 for HD4-A-LT and HD4-B-LT. The calculation results suggest the screech instability occurred at relatively low two-phase density early in the start sequence.

As described in the previous section, using the measured value of flow-rate from the turbine flowmeter, Q, is clearly not ideal in the analysis since the primary area of interest is the startup timeframe. However, since the points of interest for this analysis occur after the initial flowmeter surge (the injector manifold fill transient), and all flowmeter data after that point is directly proportional to the measured chamber pressure, the flowmeter data is reliable enough to draw general conclusions requiring known mass flow. Hence, some insight into the injector behavior can be gained by using this data.

2. Two-Phase Injection Velocity - Hewitt Stability

The calculated two-phase propellant density, $\rho_{2\phi}$, was used to calculate a two-phase injection velocity, $v_{2\phi}$, with Equation 1. Figure 20 shows the two-phase injection velocity calculation results for HD4-A-LT and HD4-B-LT. Note that unstable tests typically occur at high methane injection velocities. Some tests suggest a possible high-LOX injection velocity triggering, though, which could explain the observed "warm LOX" instability.

In order to perform a stability characterization for the Hewitt d/v parameter, the Hewitt plot from Hulka and Hutt[12] was modified from the oxygen-hydrogen curve to a oxygen-methane curve. The chamber diameters were scaled by the difference of the sound speeds, assuming oxygen methane hot gas sound speed is 3,600 ft/sec. The resulting Hewitt stability characterization is shown in Figure 21. Although Hulka and Hutt did not show a 1R characteristic limit, a 1R estimate is included in Figure 21 for comparison.

The limits established for two-phase injection velocity triggering of the instabilities from Figure 20 were used to characterize d/v. As shown in Figure 21, instabilities trigger when the fuel core and barrier elements cross the 1R estimate (nealy coincident with the 3T estimate). The oxygen limits from Figure 20 do not make an obvious boundary limit for d/v, but may indicate a possible trigger when the LOX core elements reach the 1T estimate.

The conclusions for fuel and LOX d/v limits are not strict, and many assumptions were required in the two-phase density / injection velocity analysis to obtain the result. However, the data do show a possible explanation of the triggering mechanism seen in the Morpheus main engine testing.

VI.   Conclusions

The Morpheus main engine test and vehicle flight campaigns at JSC, SSC, and KSC successfully demonstrated a fully integrated LOX/methane propulsion system. Integrated main engine and RCE testing and flight operations were demonstrated. Main engine testing successfully demonstrated 4:1 throttling, enabling

American Institute of Aeronautics and Astronautics
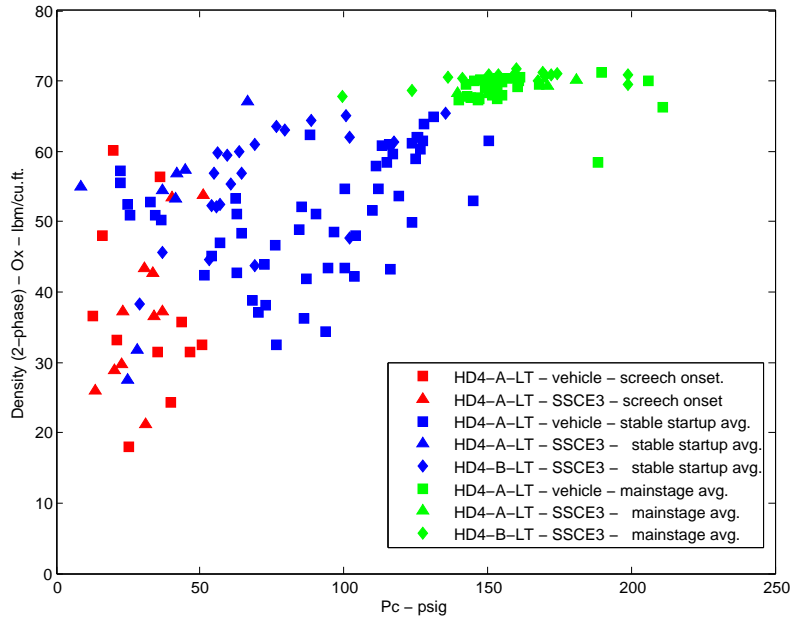
(a)
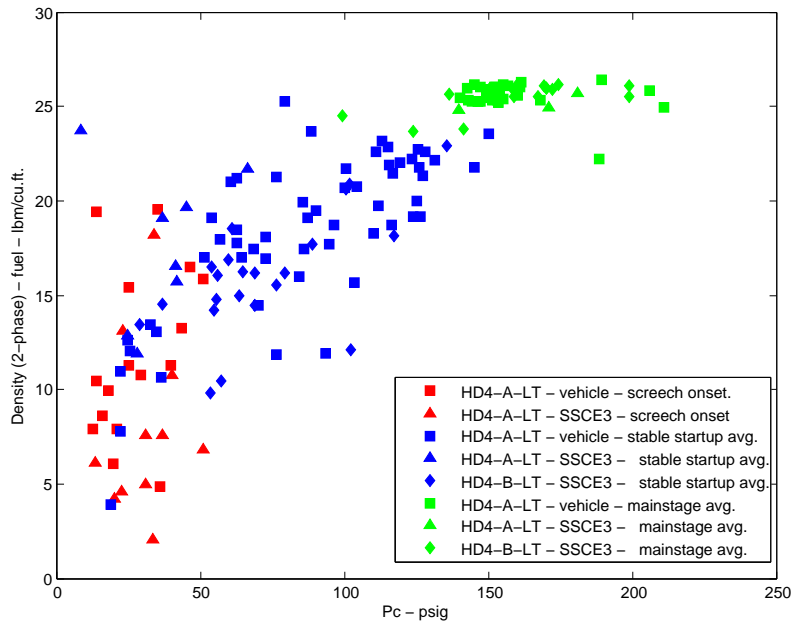
(b)

Figure 19. Calculation results for two-phase propellant density, $\rho_{2\phi}$, plotted against Pc for HD4-A-LT and HD4-B-LT. (a) LOX injector. (b) LCH4 injector.

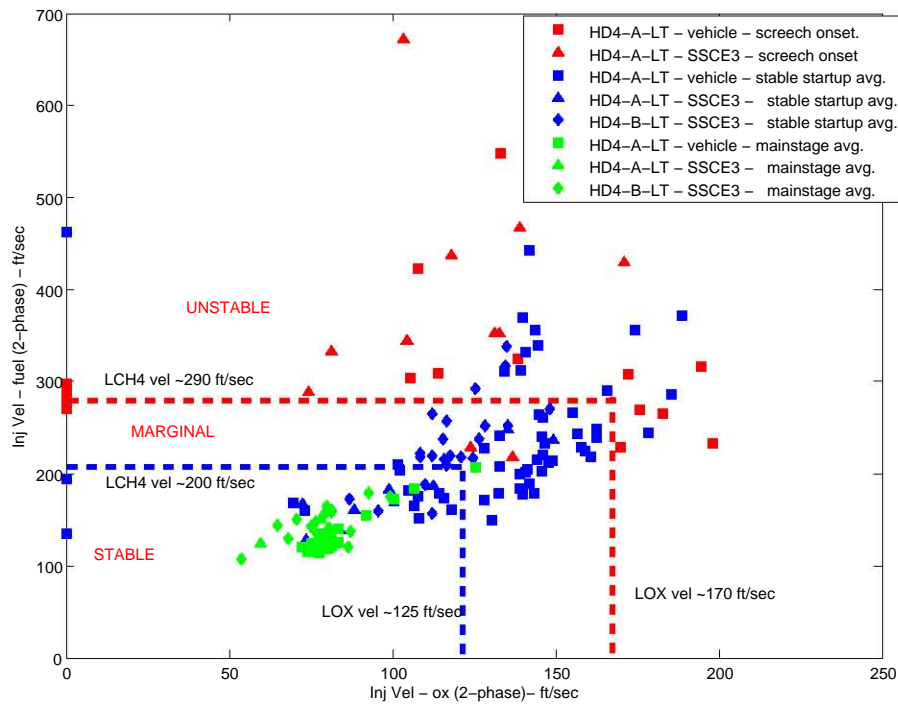American Institute of Aeronautics and Astronautics

Figure 20. Calculated two-phase injection velocities of HD4-A-LT and HD4-B-LT. Unstable tests primarily occur high methane injection velocities, with some tests indicating a potential high-LOX injection velocity trigger. Note tests shown as zero LOX velocity had failed flowmeter.
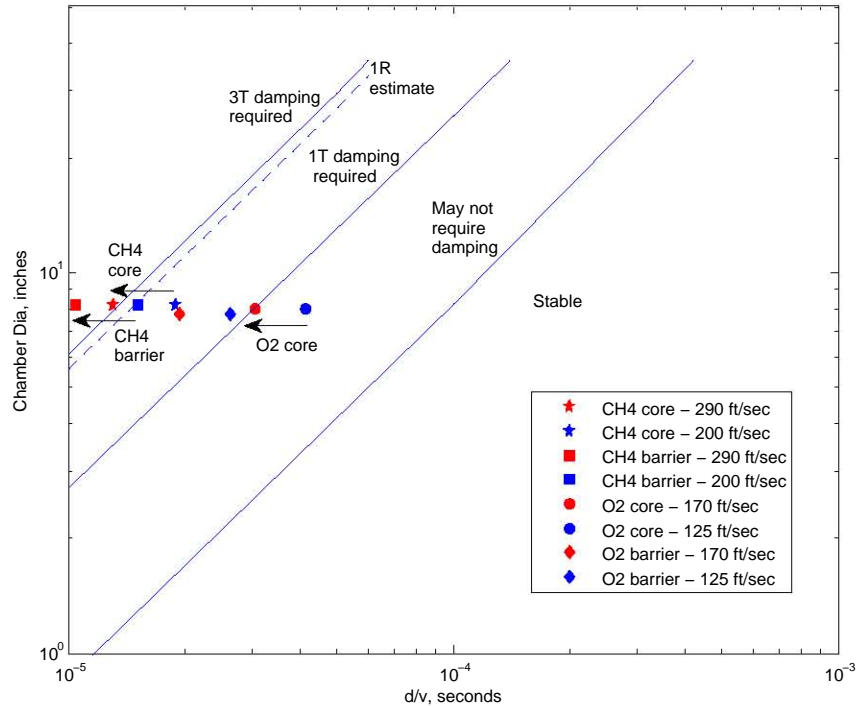

Figure 21. Hewitt stability characterization for HD4, figure adapted from Hulka and Hutt,[12] scaled for oxygen-methane sound speed. Two-phase calculated d/v operating limits established in Figure 20 show that instabilities trigger when the fuel core and barrier elements cross the 1R estimate. The oxygen limit may indicate a trigger when the LOX core elements cross the 1T estimate.

American Institute of Aeronautics and Astronautics

vehicle lander operations. Notably, ignition instability was overcome using updated start procedures. Major observations and conclusions regarding chug and screech combustion instabilities are as follows:

A. Major Test Observations

1. Test Observations: Chug Stability

- Chug instability was never observed during mainstage throttling, and 4:1 throttling was successfully demonstrated.

- Injector pressure drop, $\Delta P/Pc$, was maintained high by use of the ball-valve for throttling maintaining a pressure cushion in the injector above the vapor pressure.

- Chug instability on the vehicle was only observed during shutdown at low Pc, just below the 4:1 throttle point at a maximum $\Delta P/Pc$ ~9-15% psid/psia.

- Chug during engine shutdown was only observed with ground or flame trench interaction acoustics.

2. Test Observations: High-speed (Screech) Combustion Stability

- High-speed (screech) combustion instabilities were observed on both the vehicle and the SSC-E3 testing.

- Screech combustion instability was never observed to initiate during mainstage engine operations and throttling.

- Instabilities typically initiated during engine startup (almost immediately following the fuel injector fill indicated by the fuel manifold thermocouple), and if the engine was subsequently throttled up, the instability would decay. However, tests at SSC-E3 did demonstrate the capability of the screech instability to propagate into mainstage.

- Over-chilled fuel inlet conditions typically caused the worst instabilities (1T, 1R, 1T1R, etc.) at engine start. Less-severe combustion instabilities could be triggered by "warm LOX" inlet conditions. The "warm LOX" instabilities appeared as 1T-1L or 1R (with harmonics) and dampen out once the LOX injector chills in.

- Screech combustion instability on the vehicle was aggravated by ground interaction acoustics which appear to mechanically ring the engine bell.

- The preponderance of the evidence suggests that the 3 kHz - 6 kHz - 9 kHz pattern is not the L modes, but definitive method of proof would require a test campaign with a different length chamber (not performed).

- Data analysis from the vehicle showed that the instability was worsened by low Pc engine startup conditions. Combustion stability during engine start was improved by optimizing the maximum allowable Pc.

- Combustion stability during engine start was improved by implementing a "cold LOX" and "warm methane" startbox that provided an effective LOX lead and higher mixture ratio start.

B. Conclusions from Data Analysis

- Although it is likely that the injector orifices are experiencing hydraulic flip during the injector chill-in and engine startup, an abrupt change in calculated C_d was not discernable due to use of the transient turbine flowmeter data and two-phase flow density variations.

- Calculation results suggest the screech instability occurred at relatively low two-phase density early in the engine start sequence.

- Unstable tests typically occurred at high fuel injection velocities calculated with two-phase density, and some tests suggest a possible high-LOX injection velocity triggering.

- Two-phase calculations for d/v suggest that the instabilities trigger when the fuel core and barrier elements cross the 1R (or 3T limit). The oxygen limits may indicate a possible trigger when the LOX core elements reach the 1T boundary.

Acknowledgments

References

[1]Devolites, J., Olansen, J. B., and Munday, S., "Morpheus 1.5a Lander Failure Investigation Results", AIAA 2013-5358, AIAA SPACE 2013 Conference and Exposition, San Diego CA, September 10-12, 2013.

[2]Olansen, J. B., Munday S., Devolites, J., and Baine, M., "Project Morpheus: Lessons Learned in Lander Technology Development", AIAA 2013-5310, AIAA Space 2013 Conference and Exposition, San Diego, CA, September 10-12, 2013.

[3]Hurlbert, E., McManamen, J. P., and Studak, J. W., "Advanced Development of a Compact 5-15 lbf Lox/Methane Thruster for an Integrated Reaction Control and Main Engine Propulsion System", AIAA 2011-6113, 47th AIAA/ASME/SAE/ASEE Joint Propulsion Conference and Exhibit, San Diego, CA, July 31-August 3, 2011.

[4]McManamen, J. P., and Hurlbert, E., "Development and Flight Operations of a 5 to 20 lbf O2/ Roll Control Engine for Project Morpheus", 50th AIAA/ASME/SAE/ASEE Joint Propulsion Conference, Cleveland, OH, July 28-30, 2014.

[5]Morehead, R. L., "Project Morpheus Main Engine Development and Preliminary Flight Testing", AIAA 2011-5927, 47th AIAA/ASME/SAE/ASEE Joint Propulsion Conference and Exhibit, San Diego, CA, July 31-August 3, 2011.

[6]Yang, V., Wicker, J. M., and Yoon, M. W., "Acoustic Waves in Combustion Chambers", *Progress in Astronautics and Aeronautics*, Vol. 169, Yang, V., and Anderson, W. E., eds., pp. 357-376, AIAA, Washington, D.C., 1995.

[7]Harrje, D. T., and Reardon, F. H., eds., "Liquid Propellant Rocket Combustion Instability", NASA SP-194, Washington, D.C., 1972.

[8]Gill, G. S., and Nurick, W. H., "Liquid Rocket Engine Injectors", NASA SP-8089, NASA Lewis Research Center, Cleveland, OH, 1976.

[9]Valentine, R. S., Rossi, F. S., and Kromrey, R. V., "Fluid Dynamic Effects on Apollo Engine Pressure Spikes", *Journal of Spacecraft*, Vol. 5, No. 1., pp. 31-35, 1968.

[10]Nurick, W. H., Ohanian, T., Talley, D. G., and Starkey, P. A., "Impact of L/D on 90 Degree Sharp-Edge Orifice Flow with Manifold Passage Cross-Flow," AFRL-PR-ED-JA-2007-256, Air Force Research Laboratory, Edwards AFB, CA, 2007.

[11]Anderson, W. E., Ryan, H. M., and Santoro, R. J., "Impinging Jet Injector Atomization", *Progress in Astronautics and Aeronautics*, Vol. 169, Yang, V., and Anderson, W. E., eds., pp. 215-246, AIAA, Washington, D.C., 1995.

[12]Hulka, J., and Hutt, J. J., "Instability Phenomena in Liquid Oxygen / Hydrogen Propellant Rocket Engines", *Progress in Astronautics and Aeronautics*, Vol. 169, Yang, V., and Anderson, W. E., eds., pp. 39-71, AIAA, Washington, D.C., 1995.

[13]Muss, J. A., "Instability Phenomena in Liquid Oxygen / Hydrocarbon Rocket Engines", *Progress in Astronautics and Aeronautics*, Vol. 169, Yang, V., and Anderson, W. E., eds., pp. 73-88, AIAA, Washington, D.C., 1995.

[14]Collier, J. G., and Thome, J. R., *Convective Boiling and Condensation*, 3rd edition, Clarendon Press, Oxford, 1996.